

Numerical study of oxy-fuel combustion behaviors in a 2MWe CFB boiler

You Ra Gwak*, Jin Han Yun**, Sang In Keel**, and See Hoon Lee*[†]

*Department of Mineral Resources and Energy Engineering, Jeonbuk National University,
567, Bakje-daero, Jeonju-si, Jeollabuk-do 54896, Korea

**Environment System Research Division, Korea Institute of Machinery and Materials,
156, Gajeongbuk-ro, Yuseong-gu, Daejeon 34103, Korea

(Received 2 April 2020 • Revised 5 June 2020 • Accepted 8 June 2020)

Abstract—Using modified IEA-CFBC (International Energy Association-Circulating fluidized bed combustion) model, a 2 MWe oxy-fuel CFBC boiler is simulated and analyzed as a promising solution to reduce greenhouse gas emission from coal power plants. This study evaluated and compared the oxy-combustion characteristics of various coals. Also, the effects of CO₂ concentration (71-79 vol%), bed temperature (850 °C) and coal properties on combustion efficiencies, CO₂ concentration, acid gas emissions were analyzed. Because of their higher N₂ and S content, sub-bituminous and bituminous coals were found to have SO_x and NO_x concentrations higher than those of anthracite. These simulation results from Oxy-fuel CFBC simulation of various coals can be used as operating parameters for design and development of commercial Oxy-fuel CFBC boilers.

Keywords: Circulating Fluidized Bed, Oxy Combustion, Anthracite, Coal, Computational Simulation

INTRODUCTION

Global energy demands have continued to increase owing to industrial and societal development over the past 25 years. Inevitably, increased energy demand has resulted in the consumption of more fossil fuels, including coal, oil, and natural gas, because they remain cheaper than renewable energy and the infrastructure for their production, distribution, conversion, and consumption is solid and stable in most countries [1-3]. Although lignite and anthracite coals contain high levels of moisture or ash and have relatively low calorific values compared with bituminous or sub-bituminous coals, there have been many active developments in the use of lignite and anthracite coals, which have abundant reserves throughout the world and are less expensive than other fuel sources. Hence, many countries with insufficient energy resources have focused on making use of more abundant and cheaper energy resources, with Korea being a case in point [4,5].

In the power generation sector, coal has been widely used via pulverized coal combustion (PCC), bubbling fluidized bed combustion (BFBC), and circulating fluidized bed combustion (CFBC). In particular, low grade coal has been used in CFBC boilers worldwide, in spite of its disadvantages, including its lower calorific value, complicated handling process, and increases in combustor size and construction costs [6-8]. CFB boiler technology has become increasingly efficient, has gained larger capacity, and is available in many countries. Following the successful commercial operation of 300 MW grade boilers in China and Europe, their availability and deployment have increased sharply [6]. In recent years, anthracite coals with high ash content or brown coal with high moisture content

have been regarded as economical fuels for them.

Since power generation relies so heavily on PC or CFB power stations, CO₂ emissions resulting from coal combustion have increased CO₂ concentration in the atmosphere, causing changes in global climate and increasing the earth's temperature and sea level. As a result, many countries have been attempting to reduce greenhouse gas emissions from fossil fuels [1], including the development of CO₂ capture and storage (CCS) technologies divided into pre-combustion, post-combustion, and oxy-fuel combustion for fossil power plants. Oxy-fuel combustion in particular can minimize the energy conversion penalty and CO₂ carbon capture avoidance and can also be applied to existing power plants as well as new ones [9,10].

The term "Oxy-fuel CFBC" technology refers to the application of pure oxygen-fired combustion to existing CFB and CCS technologies. Oxy-fuel CFBC has been evaluated as suitable for global power generation because it has the advantages both of CFB technology and oxy-fuel combustion. For this reason, in addition to lab-scale studies of pure oxygen, CFB boiler technology studies have also attempted to gradually increase its scale to 30 MWth scale oxy-fuel CFBC processes [4,10-18]. The studies performed so far, however, have involved only lab-scale or pilot-scale plants mostly using bituminous coals [6,18]. Moreover, the operating performance and characteristics of oxy-fuel CFBC change in response to external factors such as fuel supply volume, gas injection volume, and operating temperature.

Under such circumstances, in order to reduce operating loss and achieve optimal performance, it is necessary to identify the dynamic behavior and predict the performance of oxy-fuel CFBC operation. Moreover, as operating conditions change, an optimal operating environment must be maintained; identifying unexpected operational changes or in-operation problems is essential. There is thus

[†]To whom correspondence should be addressed.

E-mail: donald@jbnu.ac.kr

Copyright by The Korean Institute of Chemical Engineers.

a need for studies of simulation tools that can predict oxy-fuel CFBC operation and respond immediately to any problems that may occur during operation. In addition, numerical simulation of oxy-fuel CFBC plays an important role in experimental result analysis as well as reactor-design verification [18].

Numerous studies have been conducted on simulation tool development for fluidized bed boiler analysis, including IEA-CFBC model, Barracuda, Fluent and so on. The IEA-CFBC model in particular describes the phenomena taking place in a CFBC boiler, including gas and solid-gas flows, the development of particle size distribution, coal conversion, homogenous and catalytic gas reactions, and heat transfer to membrane walls and tube bundles. The IEA-CFBC model has advanced from 1-dimensional (1D) modeling, which considered only the axial direction, to 1.5D modeling, which considers elements of both radial and axial directions (core and annulus) [6,19,20-23]. In particular, considerable efforts have been devoted to analyzing CFBC processes by applying 3-dimensional (3D) computational fluid dynamic (CFD) models such as Barracuda and Fluent [18,24-26]. However, 3D modeling presents many difficulties regarding flow analysis and reaction testing because it takes a long time to calculate, requires high specification equipment, and its grid is limited. Due to the extended time period it requires for calculating reaction and analyses, 3D modeling is of limited utility for immediate response to on-site problems. By contrast, because calculations for the IEA-CFBC model can be completed within shorter time periods, they are preferable for on-site applications [6,19,20]. Though there are some prior studies for oxy-fuel CFBC, it is not enough to design commercial or pilot scale oxy-fuel CFBC boiler for anthracite or sub-bituminous coals.

In this study, a simulation tool based on the IEA-CFBC model was developed to analyze the operating characteristics of pure oxygen CFB boilers in oxy-fuel CFBC. To investigate the effects of changes in CO₂ content and bed temperature, additional analysis was performed using fixed amounts of anthracite with high ash content, as well as both sub-bituminous and bituminous coal, while only CO₂ was assumed to be recirculated. The study's objective was for its findings to be used as guideline data for CFB boiler operation under both air-fired and oxy-fired conditions. Especially, the results from this study could be used as design values for the development of commercial oxy-fuel CFBC boiler for anthracite or sub-bituminous coals.

MODIFIED IEA-CFBC MODEL FOR OXY-FUEL CFBC

1. IEA-CFBC Model

The simulation model used in this study was a modified and developed version of the IEA-CFBC model. The 1.5D CFBC modeling program was developed by the modeling group within the fluidized bed committee under the International Energy Agency (IEA) to describe the phenomena occurring in a CFBC boiler, including gas and solid-gas flows, the development of particle size distribution, coal conversion, homogeneous and catalytic gas reactions, as well as heat transfer to membrane walls and tube bundles [19,20]. Until now, the IEA-CFBC model has been successfully used in the design and evaluation of a variety of CFBC boilers, from a 100 kW pilot-scale CFBC to a 600 MWe commercial CFBC boiler

[6,7,19,20]. As a means of predicting combustion phenomena in a CFBC boiler, the IEA-CFBC model uses a number of fields for the interdependent mechanical, chemical, and thermal processes taking place during the CFBC process. Processes that can be calculated and analyzed have included, for example, the fluidization pattern of solid flow, changes in the particle size distribution of solid materials, gas flow and composition with boiler height, combustion characteristics of coal, homogeneous and heterogeneous gas reactions, and heat transfer.

2. A Modified IEA-CFBC Model for Oxy-fuel CFBC

To simulate and analyze the oxy-fuel combustion characteristics of various coals in this study, we modified the IEA-CFBC model. In oxy-fuel combustion, pure oxygen and recycled flue gas consisting mostly of CO₂ are used in place of air. For this reason, the density, viscosity, constituents, and thermal conductivity of reactant gas mixtures are likely to change. These changes in turn can affect overall phenomena such as fluidization states, solid fraction, temperature gradients, heat transfer, combustion, gas composition, and so on.

Accordingly, certain gas properties and operation sub-routines such as density, viscosity, and thermal conductivity were modified based on previous equations [27-31]. Gas input was also modified since flue gas has to be reinjected in case of oxy-fuel CFBC operations. In the case of density, the formula shown below was based on existing research data for the calculation of $\rho_{g,0}$ (1 bar, 273 K), and was used to calculate and apply values with various O₂ mixing percentages:

$$\rho_{g,0} = \frac{[P \times (\text{O}_2, \text{mole weight} \times \text{O}_2, \%)] + [P \times (\text{CO}_2, \text{mole weight} \times \text{CO}_2, \%)]}{R_g \times T(\text{K})} \quad (1)$$

The equations for viscosity were based on those proposed by Crane company [27] and Weast et al. [28]:

$$\mu_g = \mu_0 \times (a + b) \times (T + T_0)^{3/2} \quad (2)$$

$$a = 0.555T_0 + C \quad (3)$$

$$b = 0.555T + C \quad (4)$$

In the case of thermal conductivity, the results from studies including those of Lemmon et al. [29], Faghri et al. [30], and Incropera et al. [31] were mathematized and applied to the simulation as follows:

$$\lambda_g = 0.00008 \times [(T - 86.25) \times \text{CO}_2, \% + (T + 32.5) \times \text{O}_2, \%] \quad (5)$$

Table 1 summarizes the gas properties calculated using these equations. The operating characteristics of a variety of coals in an oxy-fuel CFBC boiler were analyzed using the modified code. In this simulation, the boiler temperature was controlled by an external heat exchanger (EHE), so there was little temperature change in the lower section of the furnace.

Table 1. Mixture gas properties calculated from Eqs. (1)-(5) at 850 °C

	Viscosity (10 ⁻⁵ kg/ms)	Density (kg/m ³)	Thermal conductivity (W/mK)
Air	4.579	0.019	0.073
Oxy 1	4.501	0.028	0.063
Oxy 2	4.577	0.027	0.064
Oxy 3	4.653	0.026	0.065

Table 2. Geometry of the combustor and cyclone of the 2 MW oxy-fuel CFBC boiler

Section	Component	Size (m)
Combustor	^① Bed area	0.8×2.4
	^② Freeboard	1.2×2.4
	^③ Total height	19.1
Cyclone	^④ Total height	6.40
	^⑤ Diameter	1.75
	^⑥ Vortex finder diameter	0.70
	^⑦ Vortex finder length	0.48
	^⑧ Inlet height	1.30
	^⑨ Inlet distance	0.88
	^⑩ Width	0.70

seal, and feeding units (coal, limestone, oxygen, air, etc.). As the schematic diagram in Fig. 2 shows, the system was designed so that the heavier materials flowing through the riser were collected by the cyclone for reinsertion via the loop seal. Table 2 provides a full summary of specific dimensions used.

2. Operation Conditions

The operation conditions for a 2 MWe oxy-fuel CFBC boiler were based on those of commercial CFBC and oxy-fuel CFBC operations [6,10,11,13-15,18-20]. Variables included O₂ mixing percentage, temperature, and coal feeding rate, as listed in Tables 3 and 4. To evaluate the effects of SO_x and NO_x discharge amounts various O₂ concentrations (21-29 vol%) were used and bed temperature was set to 850 °C, as shown in Table 3. To observe the changes in O₂/CO₂ ratios, the coal feeding rate was set to 0.24 kg/s. Because operation conditions and fuels were different and excess O₂ ratio was set to 1.2, total gas flow rates varied between 1.157 Nm³/s and 2.071 Nm³/s, as summarized in Table 4. Total gas flow was divided into primary gas flow, injected via the distributor plate at the bottom (Bed height: 0 m), and two secondary flows injected above the dense bed (1.2 m and 2.6 m above the distributor plate). The ratios of these primary and secondary gas flows were 0.66 and 0.34 respectively.

The coals used for the study were anthracite, sub-bituminous coal (KPU), and bituminous coal (BG). Table 5 shows results from both proximate and ultimate analysis. The anthracite used was sourced domestically from eastern Korea and is composed of 35.34 wt% ash, 4.04 wt% volatile matter, 3.60 wt% moisture, and

Table 3. Experimental conditions

Operating condition	Coal	Reaction temperature	O ₂ concentration	Coal feeding rate
Air fired (O ₂ /N ₂)	Anthracite	850 °C (T3)	21 vol%	0.24 kg/s
Oxy 1 (O ₂ /CO ₂)			21 vol%	0.24 kg/s
Oxy 2 (O ₂ /CO ₂)			25 vol%	0.24 kg/s
Oxy 3 (O ₂ /CO ₂)			29 vol%	0.24 kg/s

Table 4. Gas flow rates with different coals and operation conditions

	Anthracite (Nm ³ /s)	KPU (Nm ³ /s)	BG (Nm ³ /s)
Air fired (O ₂ /N ₂)	1.598	2.071	2.01
Oxy 1 (O ₂ /CO ₂)	1.598	2.071	2.01
Oxy 2 (O ₂ /CO ₂)	1.341	1.74	1.689
Oxy 3 (O ₂ /CO ₂)	1.157	1.499	1.455

Table 5. Analysis of coals and limestone

		Anthracite	KPU	BG
Ultimate analysis (wt%, as dry basis)	C	60.76	71.73	67.63
	H	0.82	4.98	4.39
	O	2.41	15.83	7.03
	N	0.43	1.2	1.55
	S	0.24	0.46	0.89
	Ash	35.34	5.80	18.51
Proximate analysis (wt%, as received basis)	Moisture	3.60	19.33	11.04
	Volatile matter	3.89	44.87	32.67
	Fixed carbon	58.44	31.12	39.82
	Ash	34.07	4.68	16.47
Limestone	Specific surface area (m ² /g)	CaCO ₃ (%)	Conversion (-)	Ca/S mole ratio (-)
	0.5095	95.6	0.19	3.0

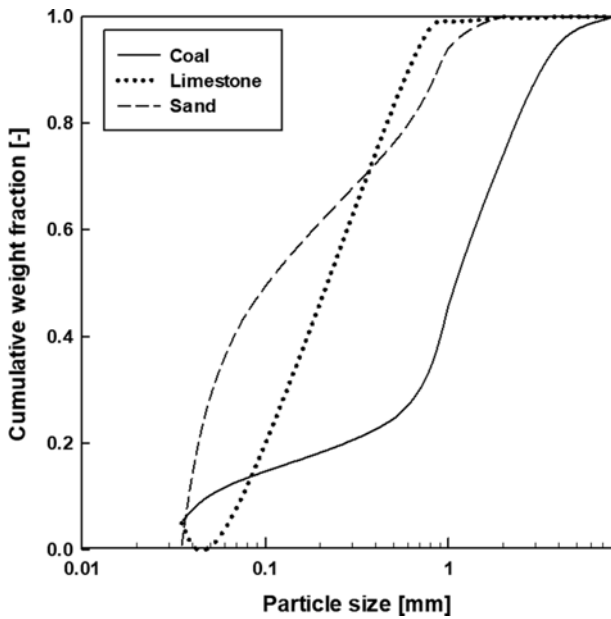


Fig. 3. Particle size distributions of coal, limestone, and sand.

60.62 wt% fixed carbon. It contains low S (0.24 wt%) and N (0.43 wt%) and has a relatively low heating value (under 19,200 kJ/kg). One of its noteworthy aspects is that it contains a small amount of water and volatile matter and a high proportion of ash compared to conventional bituminous and sub-bituminous coals. Limestone was used to remove SO_x from the flue gas; its $CaCO_3$ content and specific surface are summarized in Table 5. For the purposes of the study, the Ca/S mole ratio was set to 2.3, in accordance with previous studies [6,10,11,13-15,18-20]. Fig. 3 shows the particle size distribution (PSD) of coal, limestone, and sand, with mean particle sizes of 1,070 μm , 280 μm , and 250 μm , respectively. The particle size distributions for the anthracite, KPU, and BG are the same.

RESULTS AND DISCUSSION

1. Temperature, Pressure and Solid Fraction Profiles

The respective effects of the different coals on temperature, pressure, and solid fraction were investigated. Simulation conditions under air-fired mode and oxy-fired mode are given in Table 3. Fig. 4 shows temperature profiles for the circulating fluidized bed riser under air-fired and oxy-fuel combustion conditions at a bed tem-

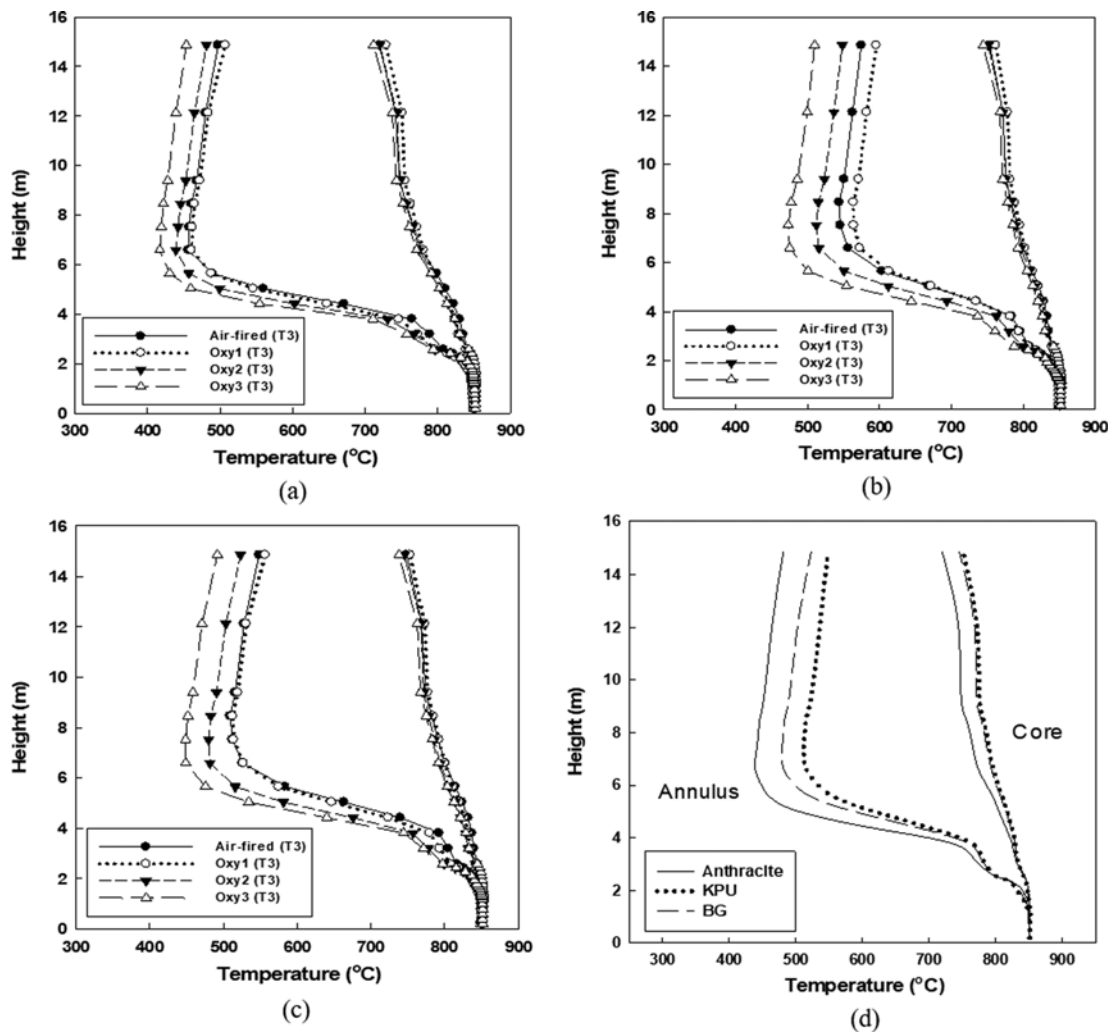


Fig. 4. Temperature profiles of three different coals. (a) Anthracite, (b) KPU, (c) BG, (d) Oxy 2 condition.

perature of 850 °C for the three types of coal. The relatively low temperature profiles on the left correspond to the annulus region of the riser, while the profiles on the right correspond to the core region. As can be seen, the bed temperature decreased in relation to increases in bed height. In the case of air-fired mode with anthracite [20], the temperature profiles in the dense region of CFB riser showed almost the same with different cyclone efficiencies, whereas it decreased gradually in the lean region of CFB riser. Lee et al. [20] reported that the temperature of the annular wall layer was lower than that of the core region and decreased in relation to increasing cyclone efficiency, because the particles were in contact with the membrane walls and flow down into the dense phase. Stanger et al. [33] maintained that an optimal temperature for air-fired CFBs is typically between 800 °C and 900 °C due to lowering SO_x and NO_x emissions, and it is expected that these operating parameters will be mostly maintained for oxy-fuel CFBs.

The temperature in the lower section of the furnace where coal is injected remained within the range of 840-850 °C with no significant differences between experiments, as shown in Fig. 4. How-

ever, the respective temperatures of the core and the annulus diverged significantly as the riser height increased. In the upper section, the temperature gradient in the annulus region was between 400 °C and 650 °C. In the core section, however, the temperature gradient was between 820 °C and 840 °C, with temperature loss occurring as the riser height increases. The temperature difference (core, annulus) between the lower and upper sections of the furnace was in the range of 70 °C-450 °C, and the temperature gradient showed a similar tendency in each case. The temperature profile of anthracite was also relatively low, while the temperature gradient of KPU coal was the highest among the three samples. This is because the combustion reaction of anthracite is relatively lower than that of sub-bituminous and bituminous coal [6,20]. BG coal showed a temperature gradient similar to that of KPU up to about 4 m, but the temperature difference between KPU and BG coal in the annulus section increased with increasing temperature. As a conclusion, the 2MWe oxy-fuel CFBC boiler had the cyclone of lower efficiency. To improve oxy-fuel combustion, the efficiency of the cyclone should be modified.

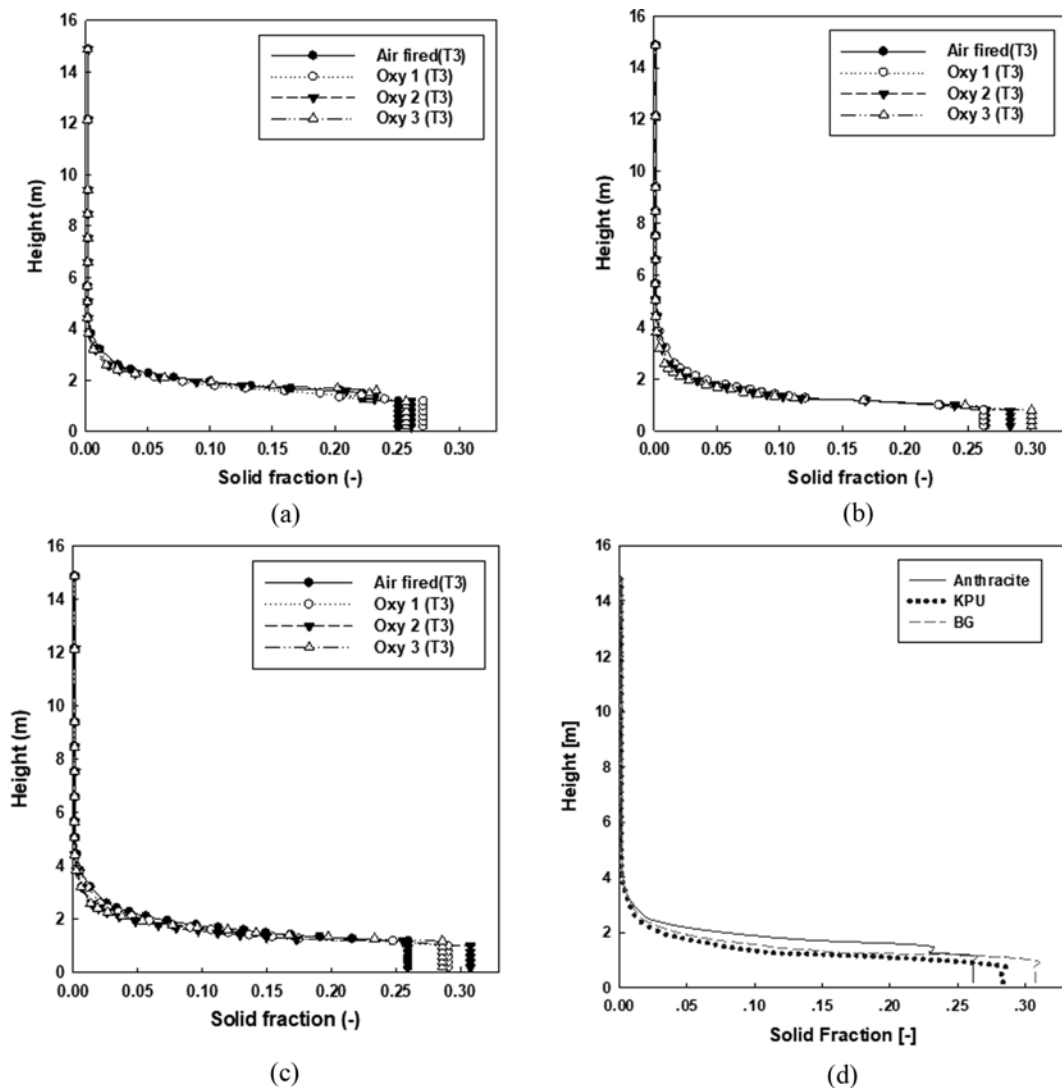


Fig. 5. Solid fraction profiles of three different coals. (a) Anthracite, (b) KPU, (c) BG, (d) Oxy 2 condition.

The predicted results for the axial solid fraction and pressure profiles in the combustor with the three different coals are shown in Figs. 5 and 6, respectively. In the dense phase the solid fractions (under 2 m above the distributor plate) varied from 0.27 to 0.32 due to the different coal properties and gas flow rates. Because the fixed carbon (or carbon content) of anthracite is lower than that of the other coals, total gas flow rates decreased, as shown in Table 4. The dense bed height thus also increased as total gas flow rates decreased. Although the high solid concentration in the dense bed helped to improve combustion efficiency, the high resistance of air permeation resulted in high power consumption by the draft fan and severe erosion of the membrane walls in the lower furnace [10,34,35]. Lee et al. [20] also reported that the dense bed height increased as cyclone efficiency increased and as the fraction of fine particles captured and circulated by the cyclone, increased in the total bed material. Moon et al. [10] reported that the solid suspension density along the riser height did not show any significant difference in either air-fired or oxy-fired mode. Comparing air-fired with oxy-fired mode, the pressure profiles for each's operation condition were almost the same. This means that the transition from air-fired to oxy-fired mode might have a lesser impact on the fluidization state in CFBCs.

Fig. 6 shows the pressure gradient under Oxy 2 conditions with different coal properties. This solid fraction variation affected the pressure profile. The pressure tends to decrease as it moves into the upper section, and the rapid decrease in pressure confirms that the region of 2 m is the dense bed. The difference in density between CO₂ and N₂ may have affected the solid density, which was analyzed as higher in the air atmosphere than the CO₂ atmosphere at the same gas flow rates [10,36]. However, the pressure of the anthracite in the dense bed was higher than that of the other coals, as Fig. 6 shows. The reason for this was the low scattering due to the small flow rate of the anthracite. In conclusion, the 2 MWe oxy-

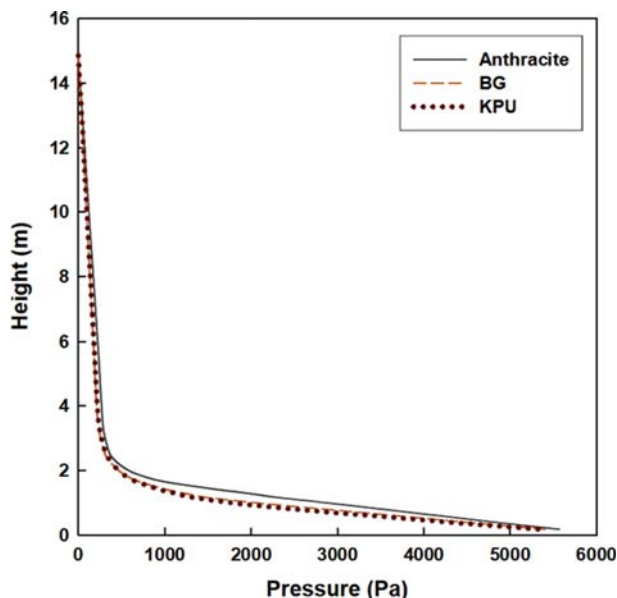


Fig. 6. Pressure profiles of three different coals in the conditions of Oxy 2.

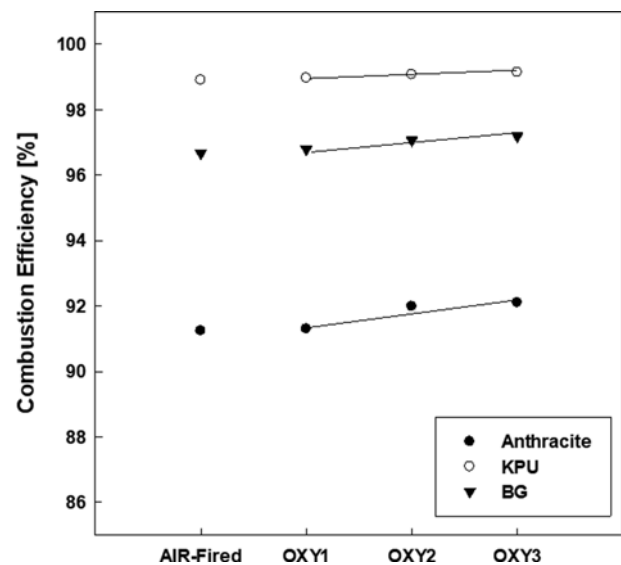


Fig. 7. Combustion efficiencies of three different coals with various conditions.

fuel CFBC boiler was determined as having the cyclone of lower efficiency. To improve oxy-fuel combustion, the cyclone's efficiency needs to be modified.

2. Combustion Characteristics

To compare the combustion characteristics of anthracite with those of other coals, we analyzed their respective combustion efficiencies, CO₂ concentrations, and acid gas concentrations under various operation conditions. The concentration of CO₂ in the flue gas of the oxy-combustion process is a particularly important factor in reducing load on the CO₂ processing unit (CPU) [4,10]. Although air ingress may be an important factor in reducing CO₂ concentration and increasing NO_x in flue gas, air ingress was not included in this simulation. Fig. 7 shows a graph of combustion efficiency in the different coal properties under various conditions. As can be seen, the combustion efficiency of the three different coals increased with increasing oxygen concentration. Stanger et al. [33] said that in oxy-fuel combustion, the gasification of char increases; thus it slightly decreases the particle temperature and combustion rate of char and the ratio of produced CO vs CO₂ is higher in oxy-fuel combustion, which is mostly due to gasification reactions. According to Bu et al. [37] the lower O₂ diffusion rate in CO₂ compared to N₂ is the main reason for the longer burnout time and lower peak temperature under oxy-fuel combustion conditions.

In the experiments using anthracite in a 90 kWth fluidized bed reactor [17], its combustion efficiency was higher in oxy-fired mode than in air-fired mode due to the higher oxygen content (30-50 vol%) and operating temperature (up to 930 °C). Moon et al. [4] reported that the overall combustion efficiency of anthracite in a 100 kWth CFBC system was 97.6%. In their experiment, the calorific value of anthracite was 22,590 kJ/kg higher than the anthracite used in the present study. In terms of combustion efficiency, KPU ranked highest and anthracite lowest under all conditions. This was because of anthracite coal's lower combustion reactivity compared to both bituminous and sub-bituminous coal. However, under air-fired conditions the difference in combustion efficiency

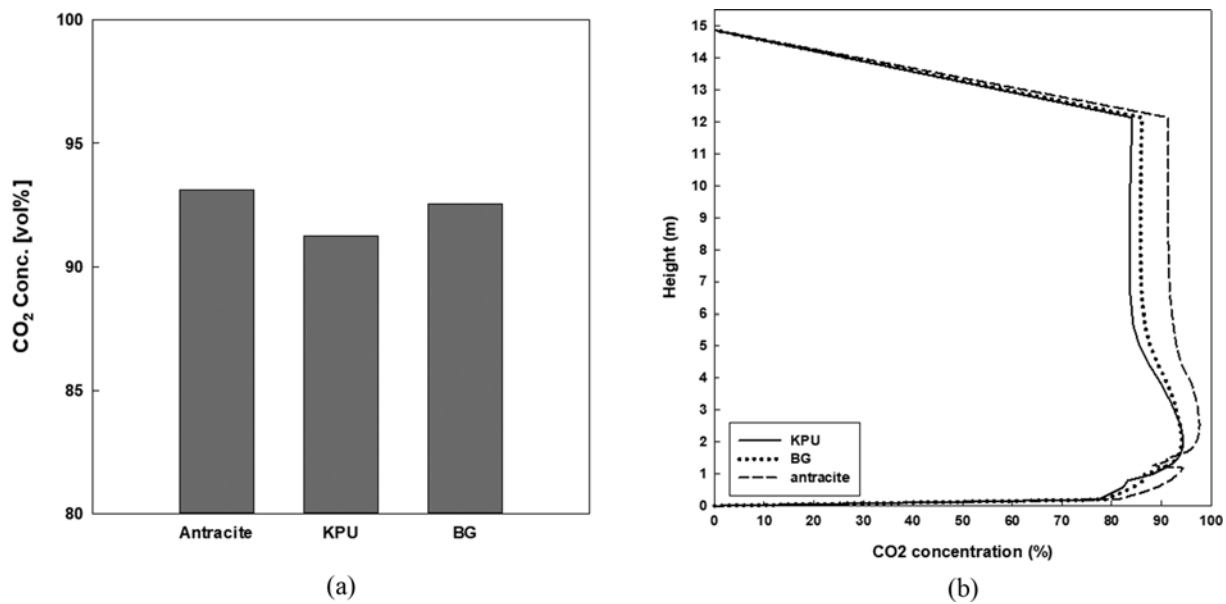


Fig. 8. The CO₂ concentration of three different coals at Oxy 2 condition. (a) CO₂ concentration/three type coals, (b) CO₂ concentration.

between KPU and anthracite is around 8%, while under Oxy 3 condition it is around 7%.

CO₂ concentration with dry-basis of three different coals at the Oxy 2 condition is shown in Fig. 8. Moon et al. [10] reported that the CO₂ purity of the flue gas used as the combustion oxidant was changed from an air atmosphere to an O₂/RFG atmosphere at the injection point and that the flue gas could achieve 96 vol% (dry basis) CO₂ levels using O₂ purity 99.999 vol%. The CO₂ concentration of anthracite under the Oxy 2 condition is 93% higher than that for both KPU and BG coal, even though the combustion efficiency of anthracite is lower than that of the other coals. As shown in Table 5, the fixed carbon component of anthracite was higher than that of KPU and BG coal. Although the combustion efficiency of anthracite was lower than that of KPU and BG coal, anthracite generated more CO₂ by reacting with residual oxygen and unreacted carbon. Thus, it was confirmed that anthracite could be used for recovering high-purity CO₂ under the oxy-fuel CFBC boiler condition. However, these results were obtained at the condition of pure oxygen and pure CO₂ recycling. In conclusion, to maintain high CO₂ concentration in flue gas it is very important that oxygen purity from the ASU and CO₂ purity in the recycling unit reach almost 100%. The increase in combustion efficiency achieved by using higher oxygen content may help in maintaining a higher CO₂ concentration in the flue gas.

Fig. 9 shows pollutant emissions such as SO₂, NO, and N₂O from three different coals experiments under oxy-fired operation conditions. The SO₂ value shown in Fig. 9 was obtained by using limestone, as shown in Table 5. Fig. 9 shows that the total emissions from anthracite are the smallest. In particular, it was confirmed that anthracite's NO_x emissions are lower than those of KPU and BG coal, while for SO_x its emissions are similar to those of KPU coal. These results confirm the findings of previous studies. SO₂ emissions from anthracite combustion are usually low, due to its sulfur content and low volatiles/char ratio [17]. However, Diez et

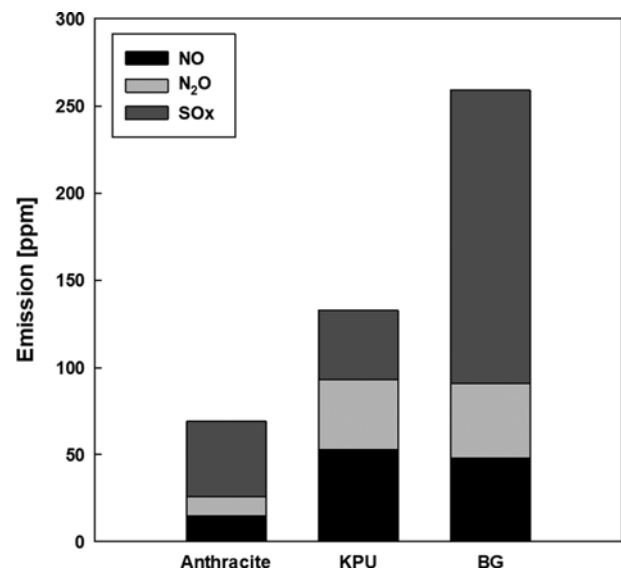


Fig. 9. SO_x and NO_x concentrations of three different coals at Oxy 2 condition.

al. [17] observed that the optimum temperature for SO₂ capture in an oxy-fuel CFBC seems to decrease as the atmosphere is enriched with O₂, because CO₂ concentration may affect the sulfation reaction path of limestone. Spörl et al. [38] said that increased SO₂ partial pressure under oxy-fuel combustion conditions stabilizes sulfates in ashes and deposits and the retention of SO₂ in the ash is improved in oxy-fuel combustion, which leads to lower energy based SO₂ emissions. Even with the increase of SO₂ levels and therefore sulfate stability in oxy-fuel combustion, SO₂ levels in oxy-fuel combustion for low sulfur coals are comparable to the concentrations experienced with high sulfur fuels in air-firing [38].

Sheikh et al. [39] suggested that oxy-fuel combustion in a fluid-

ized bed for carbon capture and minimizing NO_x emissions is highly sustainable compared to other approaches. They also suggested that both NO_x formation and fuel-N conversion have significant limitations under fluidized bed oxy-fuel combustion compared to air combustion, and that the mechanism of NO_x formation remains deficient and in need of further development. Li et al. [15] reported that NO concentration remains essentially constant, while N₂O and fuel N conversion decrease significantly as oxygen concentration increases in the primary flow, indicating that oxygen concentration in the primary flow has no significant effect on NO emission.

CONCLUSION

To compare the combustion characteristics of anthracite, a high ash content coal, with those of sub-bituminous and bituminous coals, we used a modified IEA-CFBC model for a 2 MWe oxy-fuel CFBC boiler under a wide range of O₂/CO₂ atmospheres, bed temperatures, and other operation conditions. The results showed that high ash content anthracite can be used as fuel in oxy-fuel CFBC boilers, and that its CO₂ concentration in flue gas can reach a level of over 93 vol% higher than that of other coals. The combustion efficiency of the 2 MWe oxy-fuel CFBC using anthracite was around 90-94%, about a difference of 6-7% from those using KPU and BG coals. The CO₂ concentration of anthracite in the oxy condition is thus anticipated to be applicable to greenhouse gas capture and utilization technologies. Air pollutant emissions from anthracite coal were reduced compared to KPU and BG coals. These results show that if anthracite is used in oxy-fuel CFBC combustion, it will be considerably more effective in the reduction of fine dust emissions. Although anthracite's combustion efficiency is low, if its residence time in the furnace is increased, it is judged that it will prove useful as much as bituminous coals than.

ACKNOWLEDGEMENTS

This work was supported by the Korea Electric Power Corporation RI (grant numbers R18XA06-49) and by a National Research Council of Science & Technology (NST) grant from the Korean government (MSIP) (No. CRC-15-07-KIER).

REFERENCE

1. S. H. Lee, T. H. Lee, S. M. Jeong and J. M. Lee, *Renew. Energy*, **138**, 121 (2019).
2. BP energy outlook: 2018 edition, www.bp.com/energyoutlook. (Accessed February 10, 2020).
3. Y. R. Gwak, Y. B. Kim, I. S. Gwak and S. H. Lee, *Fuel*, **213**, 115 (2018).
4. J. H. Moon, S. H. Jo, T. Y. Mun, S. J. Park and J. Y. Kim, *Korean Chem. Eng. Res.*, **57**(3), 400 (2019).
5. I. S. Gwak, Y. R. Gwak, Y. B. Kim and S. H. Lee, *J. Ind. Eng. Chem.*, **58**, 154 (2018).
6. Y. R. Gwak, Y. B. Kim, S. I. Keel, J. H. Yun and S. H. Lee, *Korean Chem. Eng. Res.*, **56**, 631 (2018).
7. J. M. Lee, D. W. Kim, J. S. Kim, J. G. Na and S. H. Lee, **35**, 2814 (2010).
8. M. Stec, A. Czaplicki, G. Tomaszewicz and K. Slowik, *Korean J. Chem. Eng.*, **35**, 129 (2018).
9. D. Y. Lee, H. J. Ryu, D. W. Shun, D. H. Bae and J. I. Baek, *Korean J. Chem. Eng.*, **35**, 1257 (2018).
10. J. H. Moon, S. H. Jo, N. H. Khoi, M. W. Seo, H. W. Ra, S. J. Yoon, S. M. Yoon, J. G. Lee and T. Y. Mun, *Energy*, **166**, 183 (2019).
11. M. Lupion, I. Alvarez, P. Otero, R. Kuivalainen, J. Lantto, A. Hotta and H. Hack, *Energy Procedia*, **37**, 6179 (2013).
12. H. I. Mathekgga, B. O. Oboirien and B. C. North, *Int. J. Energy Res.*, **40**, 878 (2016).
13. L. Jia, Y. Tan, D. McCalden, Y. Wu, I. He, R. Symonds and E. J. Anthony, *Int. J. Green Gas Control*, **7**, 240 (2012).
14. L. Duan, H. Sun, C. Zhao and X. Chen, *Fuel*, **127**, 47 (2014).
15. S. Li, W. Li, M. Xu, X. Wang, H. Li and Q. Lu, *Fuel*, **146**, 81 (2015).
16. Y. Tan, L. Jia, Y. Wu and E. J. Anthony, *Appl. Energy*, **92**, 343 (2012).
17. L. I. Diez, C. Lupianez, I. Guedea, I. Bolea and L. M. Romeo, *Fuel Process. Technol.*, **139**, 196 (2015).
18. C. Yang, Y. Kim, B. Bang, S. Jeong, J. Moon, T. Y. Mun, S. Jo, J. Lee and U. Lee, *Fuel*, **267**, 117206 (2020).
19. J. P. Hannes, *Mathematical modeling of circulating fluidized bed combustion*, PhD Thesis, Delft University of Technology, The Netherlands (1996).
20. J. M. Lee, J. S. Kim and J. J. Kim, *Energy*, **28**, 575 (2003).
21. S. Seddighi, D. Pallares and F. Johnsson, *One-dimensional modeling of oxy fuel fluidized bed combustion for CO₂ capture*, ECI Digital Archives (2010).
22. C. K. Jayarathna, B. E. Moldestad, L. A. Tokheim, *Linköping Electronic conference proceedings*, Iceland, 76-82 (2017).
23. S. Kallio, J. Ariaksinen, M. Gulden, A. Hermanson, J. Peltola, J. Ritvaanan, M. Seppala, S. Shah and V. Taivassalo, *Proceedings of Finnish-Swedish Flame Days (2009)*. http://www.ffrc.fi/FlameDays_2009/3A/KallioPaper.pdf
24. Y. Wu, D. Liu, D. Zheng, J. Ma, L. Duan and X. Chen, *Fuel Process. Technol.*, **195**, 106129 (2019).
25. L. M. Amoo, *Fuel*, **140**, 178 (2015).
26. Y. Wu, D. Liu, L. Duan, J. Ma, J. Xiong and X. Chen, *Fuel*, **216**, 596 (2018).
27. Crane Company, *Flow of fluids through valves, fittings, and pipe*, Technical Paper, Connecticut (1988).
28. R. C. Weast, *CRC handbook of chemistry and physics*, Chemical Rubber Company, Florida (1954).
29. E. W. Lemmon and R. T. Jacobsen, *Int. J. Thermophys.*, **25**, 21 (2004).
30. A. Faghri and Y. Zhang, *Transport phenomena in multiphase systems*, Elsevier, Amsterdam (2006).
31. F. P. Incropera, D. P. DeWitt, T. L. Bergman and A. S. Lavine, *Fundamentals of heat and mass transfer*, 6th Ed., John Wiley & Sons, New York (2007).
32. Future Energy Plant, <https://www.kier.re.kr/fep>. (Accessed March 20, 2020).
33. R. Stanger, T. Wall, R. Spörl, M. Paneru, S. Grathwohl, M. Weidmann, G. Scheffknecht, D. McDonald, K. Myöhänen, J. Ritvanen, S. Rahiala, T. Hyppanen, J. Mletzko, A. Kather and S. Santos, *Int. J. Greenh. Gas Control*, **40**, 55 (2015).
34. A. Gungor, *Fuel*, **87**, 1083 (2008).
35. A. M. Gyulmaliev and M. Y. Shpirt, *Solid Fuel Chem.*, **42**, 263 (2008).

36. M. Komorowski and W. Nowak, *The 14th international conference on fluidization-from fundamentals to products*, ECI Symposium Series, (2013). http://dc.engconfintl.org/fluidization_xiv/32
37. C. Bu, A. Gómez-Barea, X. Chen, B. Leckner, D. Liu, D. Pallarès and P. Lu, *Appl. Energy*, **177**, 247 (2016).
38. R. Spörl, M. Paneru, S. Babat, G. Stein-Brzozowska, J. Maier and G. Scheffknecht, *Fuel Process. Technol.*, **141**, 258 (2016).
39. K. E. Sheikh, M. J. H. Khan, M. D. Hamid, S. Shrestha, B. S. Ali, G. A. Ryabov, L. A. Dolgushin, M. A. Hussain, T. V. Bukharkina and E. A. Gorelova, *Chin. J. Chem. Eng.*, **27**, 426 (2019).